

The 2019 Full-Scale Shake Table Test Program of Wood Dwellings

T. Nagae⁽¹⁾, S. Uwadan⁽²⁾, C. Yenidogan⁽³⁾⁽⁴⁾, S. Yamada⁽⁵⁾, H. Kashiwa⁽⁶⁾, K. Hayashi⁽⁷⁾,
T. Takahashi⁽⁸⁾, T. Inoue⁽⁹⁾

⁽¹⁾ Associate Professor, Nagoya University, nagae@nagoya-u.jp

⁽²⁾ Graduate Student, Nagoya University

⁽³⁾ JSPS Fellow, Nagoya University, cem.yenidogan@gmail.com

⁽⁴⁾ Assistant Professor, Bahçeşehir University, cem.yenidogan@eng.bau.edu.tr

⁽⁵⁾ Associate, NIKKEN SEKKEI LTD, shohei.yamada@nikken.jp

⁽⁶⁾ Senior Researcher, NILIM, kashiwa-h92ta@mlit.go.jp

⁽⁷⁾ Assistant Professor, Toyohashi University of Technology, hayashi@ace.tut.ac.jp

⁽⁸⁾ Senior Researcher, NIED, takehiro@bosai.go.jp

⁽⁹⁾ Deputy Director, NIED, dinoue@bosai.go.jp

Abstract

The 2019 full-scale shake table test program of wood dwellings is addressed in this paper. The current Japanese seismic design guidelines were applied and two Grade-3 index buildings were prepared. One adopted the Post-and-Beam Structure (A-building), and the other the Shear-Wall structure (B-building). A series of tests planned very different physical boundary conditions surrounding their reinforced concrete foundations. In the first Phase 1, A-building was equipped with a base-isolation system, while B-building represented a generic foundation constructed on real soil by preparing a rigid soil box. In the second Phase 2, the foundation of A-building was firmly fixed, while cast-iron plates were installed beneath the foundation of B-building to control the friction resistance of the foundation. In the third Phase 3, the damaged first-story of A-building was retrofitted, and the foundation of B-building was firmly fixed. The two test buildings were densely instrumented with both conventional and smart sensing technologies to monitor the building's functionality. Utility pipelines were embedded in the soil and connected to the building. The damage states of structural and nonstructural systems under each boundary condition were evaluated in a sequence of multiple strong earthquakes.

Keywords: Shaking table test, Wood dwelling, Soil-structure interaction, Functionality, Base isolation

1. Introduction

The 1995 Kobe earthquake and the 2011 Tohoku earthquake caused catastrophic damage to buildings and infrastructure. Densely populated urban areas may induce even worse situations in future earthquakes. MEXT (the Ministry of Education, Culture, Sports, Science and Technology) has been leading the Metropolitan Special Project to mitigate such earthquake disasters based on unprecedented experimentations by E-Defense (the large shaking table facility) from 2005. The Tokyo Metropolitan Resilience Project was planned for the period from 2017 to 2022. A comprehensive test plan for current or future wood dwellings in densely populated urban areas was proposed in this Project (Fig. 1).



Fig. 1 A proposal for experimentation on wood dwelling systems located in densely populated urban areas

“The 2019 full-scale shake table test program of wood dwellings” is explained in this paper with the main test results. Two test buildings were designed and constructed according to the current Japanese design guidelines. A three-story wood dwelling reflected the trends of densely populated urban areas. From the viewpoint of the resiliency and functionality of such building system, the base-isolation system is expected to minimize damage to most structural and non-structural elements. However, the requirement of clearance surrounding the base isolation layer can be a serious problem in densely populated urban areas. Maximum deformation of the base isolation layer should be limited by effectively equipping oil dampers. For current normal buildings, the foundations are directly constructed on soil, and a stiff reinforced concrete flat slab has been required recently. A variety of embedded pipelines constitute the building functionality critical to earthquake resilience. Thus, a large soil box representing 1.5 m-high soil was designed for the relevant test series. The ground motions recorded during the 1995 Great Hanshin (Kobe) earthquake and the 2011 Megathrust Tohoku earthquake literally exceed the intensity levels considered in design practice. Japanese Grade-3 index buildings may provide hints to overcoming the maximum-considered earthquakes in terms of the structural and functionality aspects. Thus, a comprehensive test program was established through intense discussions concerning these current typical issues.

2. Test Building and test schedule

Two test buildings were planned to widely cover Japanese practice. One adopted the Post-and-Beam Structure (A-building), and another the Shear-Wall structure (B-building). The Post-and-Beam Structure represents the traditional Japanese structural system. The Shear-Wall structure is known as the Two-by-Four construction method and is equally utilized in Japan. Regarding design and construction, the Japanese seismic grading scheme was applied. Requirements concerning the amount of equivalent wall have been enhanced, and metal reinforcements for connections and steel anchor bolts securing the column base have been developed and strictly required in reference to the past seismic failure mechanism of wood buildings. Both the Post-and-Beam and Shear-Wall Structures have been improved from such point of view. Grade-2 and Grade-3 index buildings especially have adopted the allowable stress design with a higher design base shear force; the base shear force coefficient of 0.2 to the standard, 0.25 to the Grade-2 index building and 0.3 to the Grade-3 index building. The design criteria of the Grade-3 index building were adopted for both of the two test buildings. The strength margin of the design requirement was minimized to evaluate the capacities of both test buildings. Figure 2 shows the elevations of two test buildings. The two test buildings adopted identical configurations and plans. Thus, the earthquake resisting capacities of the upper structures of A-building and B-building were assumed to be equivalent in the design process.

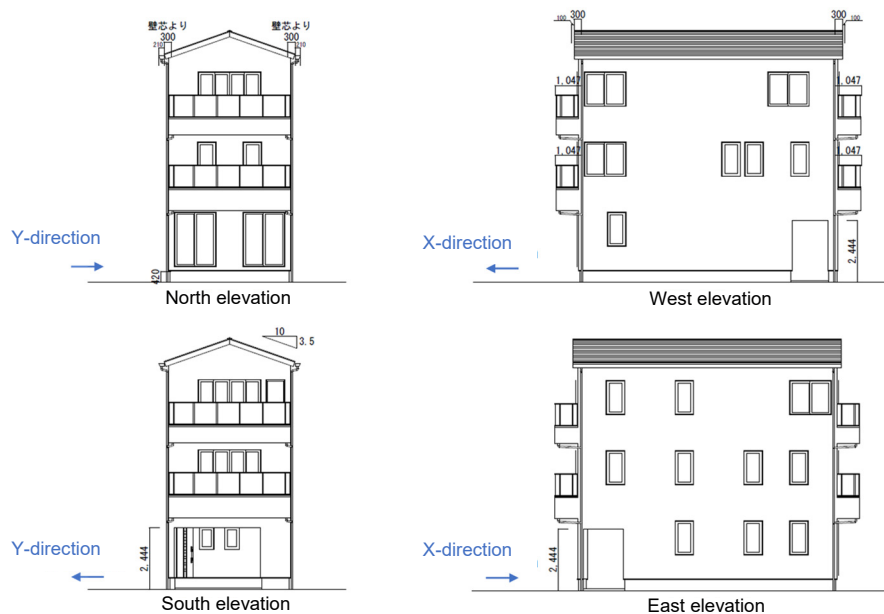


Fig. 2 Elevations of A-building and B-building

The test system of B-building accommodated real 1.5 m-high soil beneath the foundation by preparing a reinforced concrete soil box of 1.7 m (H) x 7.0 m (W) x 13.0 m (L), as shown in Fig. 3. Silica sand was utilized for the soil, and each of the five layers of 250 mm were compacted individually. Figure 4 shows the setups of A-building and B-building on the E-Defense table. Horizontally wide steel frames covered the exterior zone of the shaking table to protect the important facilities equipped inside the outer moat. The X-direction of the test buildings was set to the shorter direction of the E-Defense table.



(1) Reinforced concrete soil box (2) Compacted soil (3) Foundation constructed on the soil

Fig. 3 Construction of soil and foundation in the soil box of 1.7 m (H) x 7.0 m (W) x 13.0 m (L)

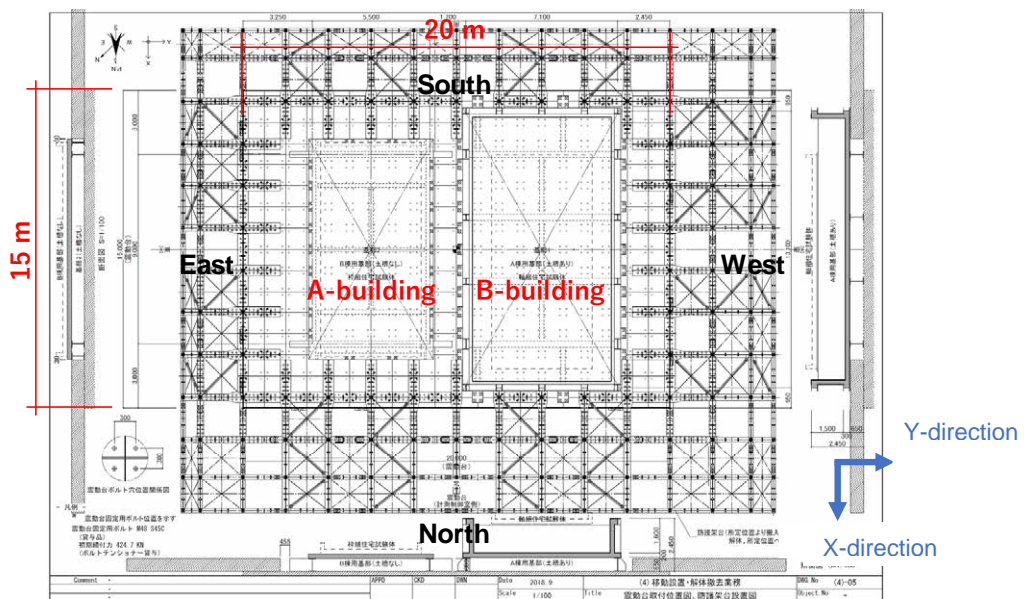


Fig. 4 Setup plan of two test buildings placed on the E-Defense shaking table

Figure 5 shows the depiction regarding the sequential tests in Phase 1, Phase 2 and Phase 3. The same upper structures were always used; the Post-and-Beam Structure of A-building and Shear-Wall structure of B-building.^[1] In the first Phase 1, A-building was equipped with a base-isolation system, while B-building represents a foundation supported on soil. The base-isolation system was composed of fifteen sliding bearings having the friction coefficient of 0.065, six laminated rubbers and six oil dampers (three for each of the X and Y-directions). The damping capacity by oil dampers was designed to fulfill a special displacement limit, supposing a densely populated urban area. In the second Phase 2, the foundation of A-building was firmly fixed, while twenty cast-iron plates were inserted beneath the foundation of B-building. The application of cast-iron plates to reduce the friction resistance of the foundation, was adopted regarding the development of an artificial input-loss system.^[2] In the third Phase 3, the first-story of A-building was retrofitted, while the foundation of B-building was firmly fixed to the rigid soil box. The test results observed in Phase 1 and Phase 2 are summarized and introduced in this paper.

Table 1 shows the input motion schedules in each Phase. The JMA-Kobe motion and JR-Takatori motion of the 1995 Kobe earthquake were used. JMA-Kobe 50% is equivalent to the Design-Based Earthquake. White noise motion tests were conducted between the ground motion tests.

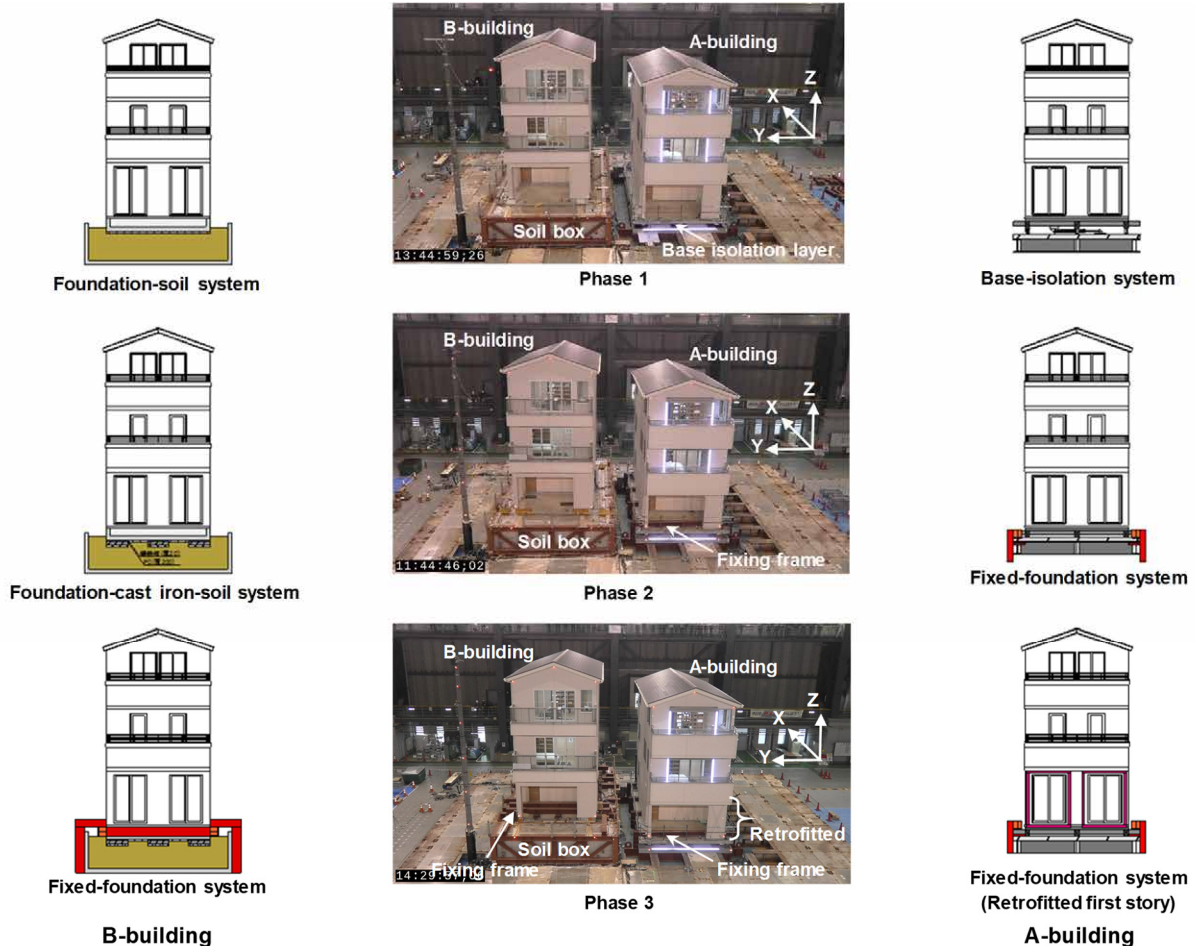


Fig. 5 Depiction regarding the sequential tests in Phase 1, Phase 2 and Phase 3

Table 1 Test schedule and input motions

Phase / Test date	Input motion	A-Building Post-Beam Structure	B-Building Shear-Wall Structure
Phase 1 January 31, 2019 February 1, 2019	(1) JMA-Kobe 25% (2) JMA-Kobe 50% (3) JR-Takatori 25% (4) JR-Takatori 50% (5) JMA-Kobe 100% (6) JR-Takatori 100%	Base-isolation system	Foundation-soil system
Phase 2 February 7, 2019	(7) JMA-Kobe 25% (8) JMA-Kobe 50% (9) JMA-Kobe 100% (10) JR-Takatori 100%	Fixed-foundation system	Foundation-cast iron -soil system
Phase 3 February 12, 2019	(11) JMA-Kobe 100%	Fixed-foundation system	Fixed-foundation system

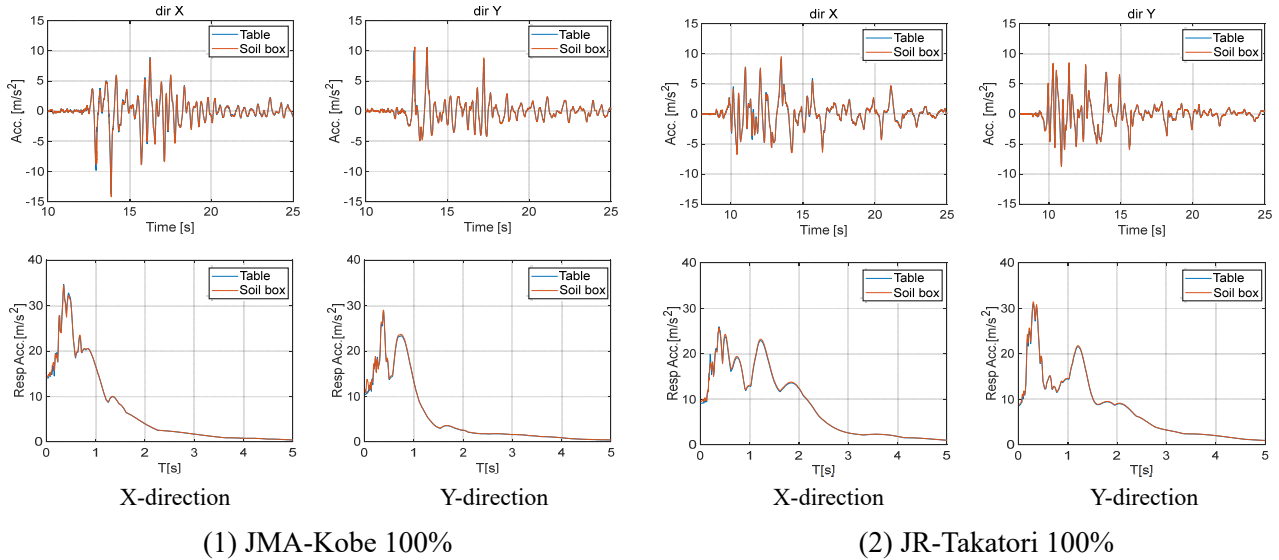


Fig. 6 Comparison of recorded motions

Figure 6 shows the recorded input motions. When subjected to JMA-Kobe 100% and JR-Takatori 100%, the evaluations became identical at the center of the shaking table and at the top of the soil box frame.

3. Test Results of A-building in Phase 1 and Phase 2

Figure 7 shows the response acceleration time histories of the third floor when A-building was subjected to JMA-Kobe 100%. Figure 7 (1) shows the base-isolation system in Phase 1, and Fig. 7 (2) shows the fixed-foundation system in Phase 2. Regarding the base-isolation system, the maximum acceleration value is one fourth of the fixed-foundation case. The maximum value is less than 4 m/s^2 in Phase 1 (base-isolation system), while more than 17 m/s^2 in Phase 2 (fixed-foundation system). Figure 8 shows the maximum floor acceleration distribution in the height. Regarding the base-isolation system, the maximum floor accelerations are the same from the first floor to the roof floor. The incrementing degree of the floor acceleration values became smaller between JMA-Kobe 100% and 50% than between 50% and 25%, although the shaking table input was increased twice between 25% and 50% as well as between 50% and 100%. This is because the developed special dampers exhibited a higher damping factor at higher velocity. In Phase 2, the maximum acceleration of the first floor is equivalent to that of the input motion, and increases two times at the upper floor.

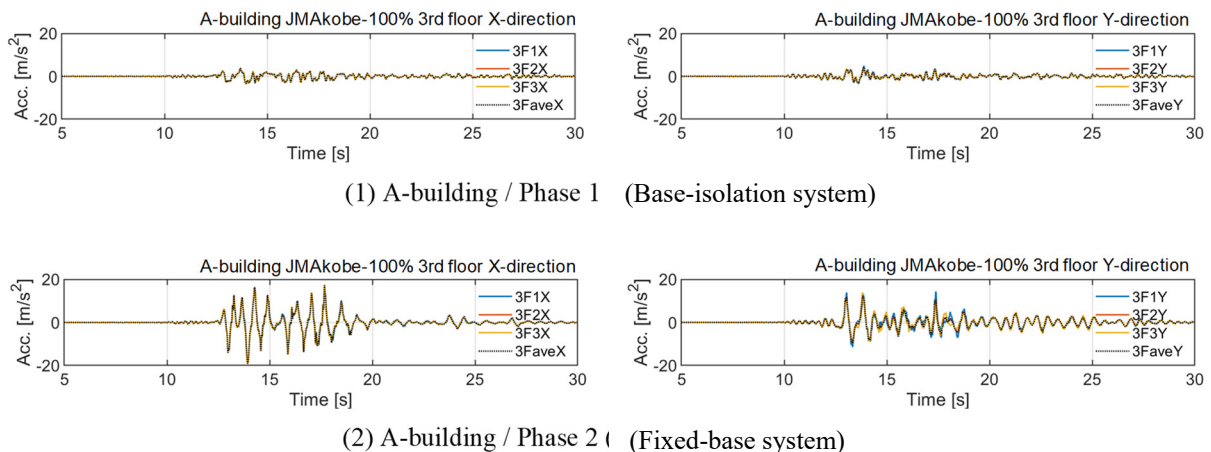
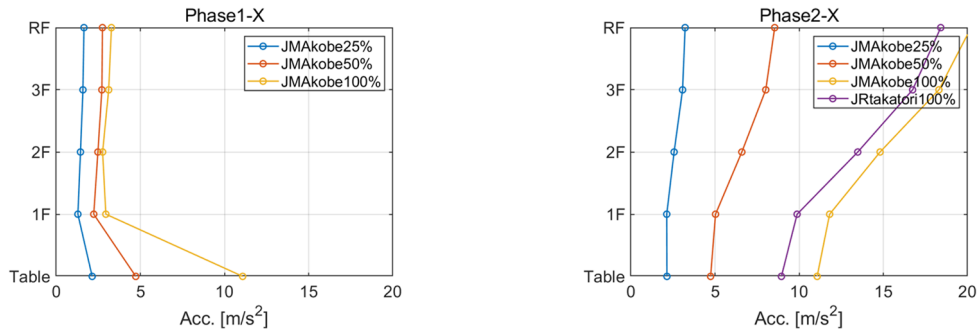


Fig. 7 Floor response acceleration time histories of A-building subjected to JMA-Kobe 100%



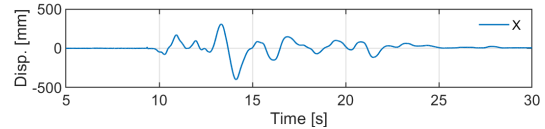
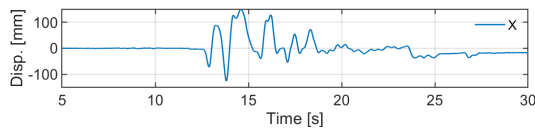
(1) A-building / Phase 1 (base-isolation system) (2) A-building / Phase 2 (fixed foundation)

Fig. 8 Maximum floor acceleration distribution of A-building (X-direction)



(1) A-building / Phase 1 (Base-isolation system) (2) A-building / Phase 2 (Fixed foundation)

Fig. 9 Damage A-building subjected to JMA-Kobe 100% (dinning room)



JMA-Kobe 100 %

JR-Takatori 100 %

(1) Displacement time history of base isolation layer (X-direction)

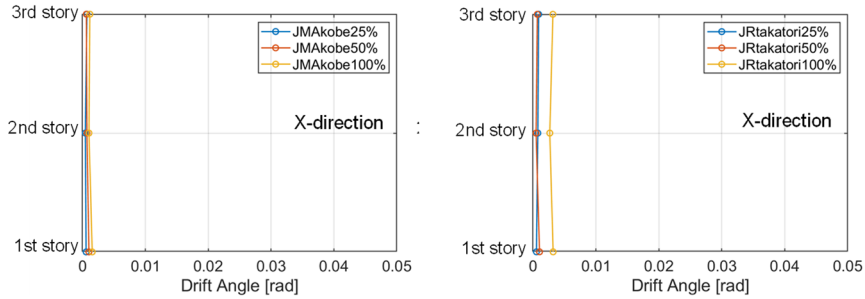


(2) Relative displacement in the base-isolation layer while subjected to JMA-Kobe 100 %

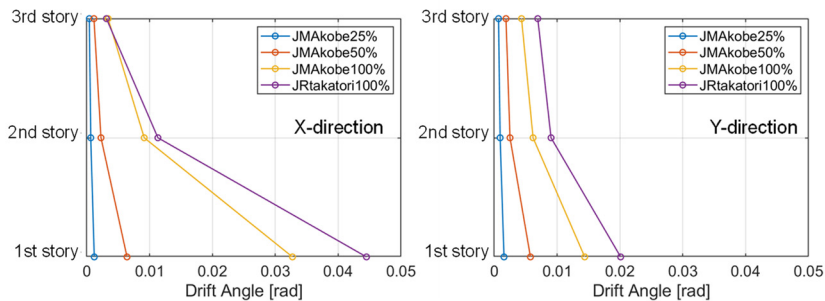
Fig. 10 Displacement time history and video capture of the base-isolation layer

The intensity of floor response is related to the damage to furniture and equipment in rooms. The test results showed significant differences between the base-isolation system and fixed-foundation system, as shown in Fig. 9. Most of the furniture overturned and was crushed in the fixed foundation case, while only one drawer of the refrigerator came open in the base-isolation case. Regarding the response of the base-isolation layer, Fig. 10 shows the relative displacement time history and snap shots of the large relative displacement.

The maximum displacement was limited to less than 150 mm during JMA-Kobe 100%. The maximum displacement slightly exceeded 400 mm during JR-Takatori 100%.

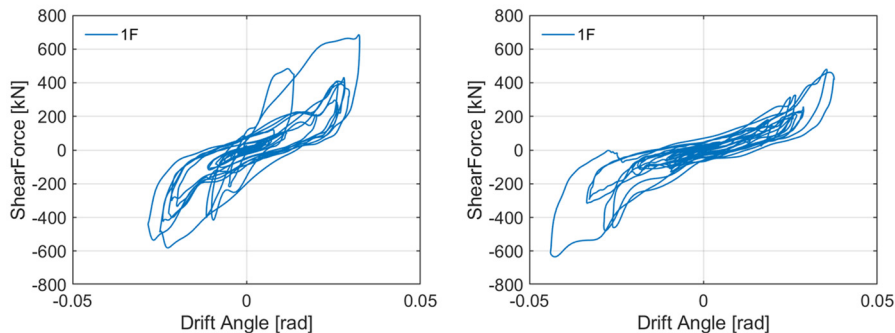


(1) Base-isolation system (A-building, Phase 1)



(2) Fixed-foundation system (A-building, Phase 2)

Fig. 11 Comparisons of the maximum inter-story drift angle distribution / A-building



(1) JMA-Kobe 100%

(2) JR-Takatori 100%

Fig.12 Relationship between story shear force and story drift angle at the first story
A-building (Fixed-foundation system) / Phase 2 / X-direction

Figure 11 (1) shows the distribution of the maximum inter-story drift angle of the base-isolation system (Phase 1). The inter-story drift angle was limited to less than 0.002 rad in JMA-Kobe 100%, and less than 0.003 rad in JR-Takatori 100%. Figure 11 (2) shows the maximum inter-story drift angle distribution of the fixed-foundation system (Phase 2). The maximum inter story drift angle was limited to less than 0.008 rad in JMA-Kobe 50%. However, when subjected to JMA-Kobe 100%, deformation of the upper structure was concentrated in the first story, and the maximum inter-story drift angle exceeded 0.03 rad. When subjected to JR-Takatori 100%, the maximum inter-story drift exceeded 0.04 rad. Figure 12 shows the relationship between the story shear force and drift angle at the first story. Peak orienting hysteretic loops were observed when

subjected to JMA-Kobe 100%, and the maximum story shear force reached 600 kN at the drift angle of 0.03 rad, which corresponded to the base shear force coefficient of 1.8. Pinching hysteretic loops were repeatedly found in the following JR-Takatori 100%, as shown in Fig. 12 (2).^[2]

4. Test Results of B-building in Phase 1 and Phase 2

A real soil boundary condition surrounding the foundation was reproduced as the test system of B-building. When the foundation-soil system was subjected to JMA-Kobe 100% (Phase 1), the maximum sliding displacement of 240 mm occurred at the foundation. The maximum sliding displacement of 300 mm occurred when subjected to JR-Takatori 100%.^[1] In the case that cast-iron plates existed beneath the foundation (Phase 2), the maximum sliding displacement became 1.3 times larger in JMA-Kobe 100%, and also 1.3 times in JR-Takatori 100%. Figure 14 shows the typical damage under the sliding displacements of the foundation. Embedded VP drain pipes had severe fractures, as shown in Fig. 14 (1). Polyethylene gas pipes showed high deformability, as shown in Fig. 14 (2), and maintained the inside pressure even after JR-Takatori 100%.

Figure 15 shows the time histories of floor response acceleration at the third floor (Phase 1). When subjected to JMA-Kobe 100% motion, the maximum acceleration values exceeded 1.0 m/s^2 . The acceleration level is two-thirds compared to the results of A-building with the fixed-foundation system, but 2.5 times larger than the results of A-building with the base-isolation system. Figure 16 shows the maximum floor acceleration

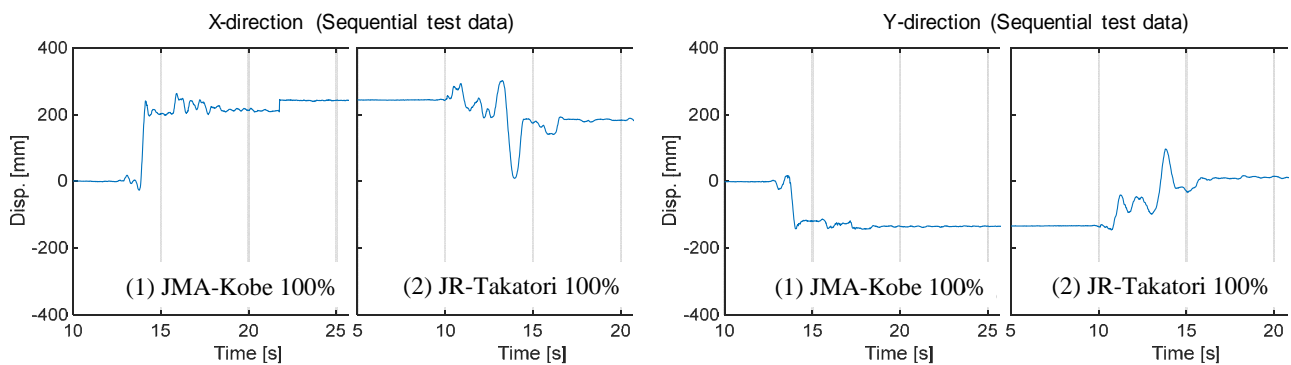


Fig. 13 Time history of foundation sliding in the sequential tests / Phase 1 (Foundation-soil system)



(1) Fractured VP drain pipe



(2) Bent polyethylene gas pipes

Fig. 14 Typical damage of pipe lines after subjected to JMA-Kobe 100% (B-building, Phase 1)

distribution in the height. The maximum floor acceleration gradually increased to the roof floor, while the maximum acceleration was slightly smaller at the first floor (foundation) than at the shaking table. As a result, furniture and equipment were significantly overturned.

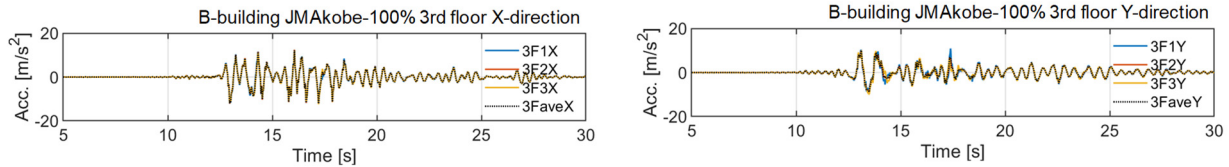
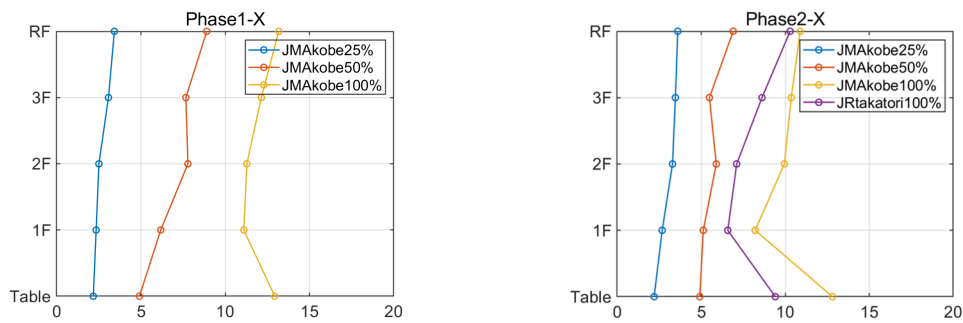


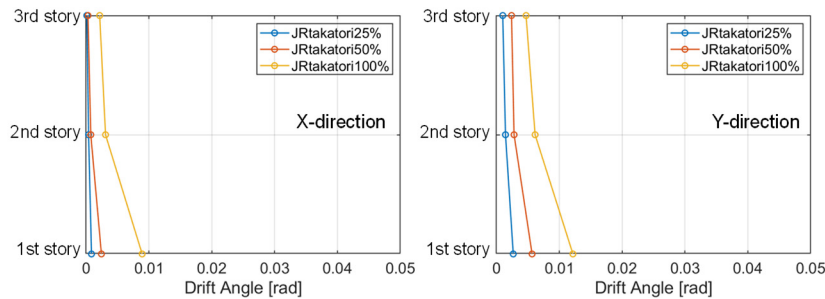
Fig. 15 B-building subjected to JMA-Kobe 100% / Phase 1 (Soil and foundation) / Comparisons of floor response acceleration time histories at the third floor



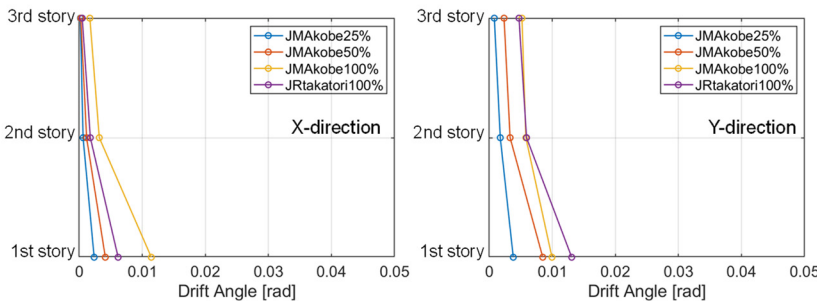
(1) Foundation-soil system (Phase 1)

(2) Foundation-cast iron-soil system (Phase 2)

Fig. 16 Maximum floor acceleration distribution of B-building / X-direction



(1) Foundation-soil system (Phase 1)



(2) Foundation-cast iron-soil system (Phase 2)

Fig. 17 Maximum inter-story drift angle distribution of B-building

Figure 17 shows the maximum inter-story drift angle distribution of B-building. The maximum inter-story drift angles were limited to less than 0.018 rad even when subjected to JMA-Kobe 100% and JR-Takatori 100% in both Phase 1 and Phase 2. As a result, the damage due to the story deformations was not significant, and minor split lines were observed on the interior walls at the first story. On the other hand, in A-building with the fixed-foundation system, the maximum inter-story drift angle exceeded 0.03 rad when subjected to JMA-Kobe 100% and exceeded 0.04 rad when subjected to JR-Takatori (Fig. 11). The upper structures of the two buildings showed comparable stiffness based on the same allowable stress design, and higher strength capacity in A-building than in B-building.^[2] The higher strength capacity of the upper structure was correspondent to the base shear force coefficient of 1.8 in A-building. On the other hand, the base shear force coefficient was limited to 1.2 in B-building with the soil-foundation system.^[1] These test results indicated that the upper structure possessing the Japanese Grade-3 capacity can induce sliding at the foundation, and result in the upper limit to seismic forces in the upper structure. Pipeline systems should be designed to accommodate sliding displacement.

5. Test Result Assessment by Acceleration Displacement Response Spectra Format

A series of tests provided a variety of results from different structural systems, such as the foundation-soil system, base-isolation system and fixed-foundation system. Significant nonlinear responses in those systems can be discussed using the Acceleration Displacement Response Spectra format, in which spectral acceleration, S_a , is plotted against spectral displacement, S_d . The Japanese seismic design code provides a consistent design route in conjunction with the code S_a - S_d spectra. The deformation distributions can be assessed given the first mode shape. Regarding the assessment of test results, the first mode shapes were defined in reference to the maximum deformation distributions. Figure 18 shows the mode vectors adopted for (1) A-building with the base-isolation system, (2) A-building with a fixed-foundation system and (3) B-building with a foundation-soil system. By using these mode vectors, the equivalent Single-Degree-Of-Freedom systems were derived.

The response assessment for the equivalent Single-Degree-Of-Freedom systems is depicted in the Acceleration Displacement Response Spectra format, as shown in Fig. 19. Figure 19 (1) shows the results of A-building with the base-isolation system. The maximum displacements correspond to S_a - S_d spectra in both JMA-Kobe 100% and JR-Takatori 100%. Figure 19 (2) shows the results of A-building with a fixed-foundation system. The maximum displacements similarly correspond to S_a - S_d spectra. Their maximum displacements of positive and negative sides are comparable in both the base-isolation and fixed-foundation systems. Figure 19 (3) shows the results of B-building with a foundation-soil system. The hysteretic characteristics induced displacement drifting to one direction with a residual displacement. Since this method assumes equal displacements on the positive and negative sides, some modifying factor may be necessary. However, the maximum displacements were quite consistent with the spectra in this test.

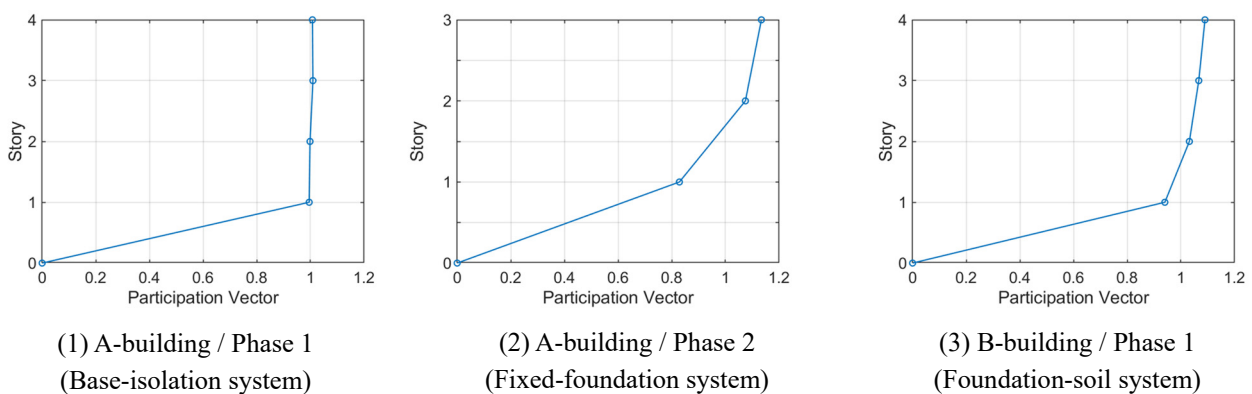
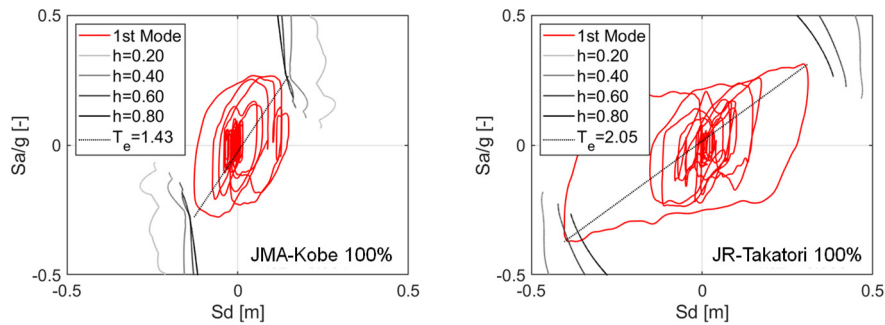
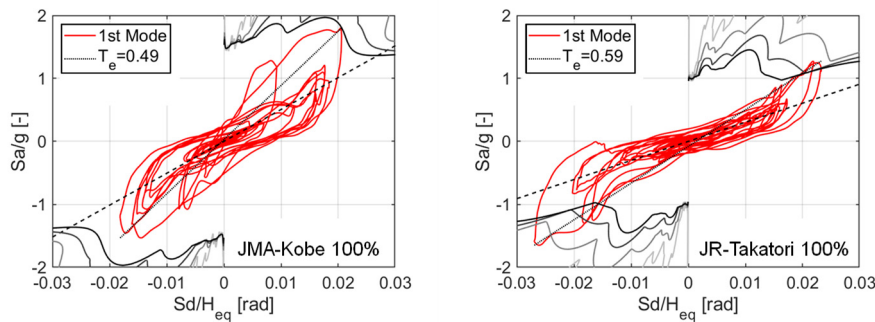


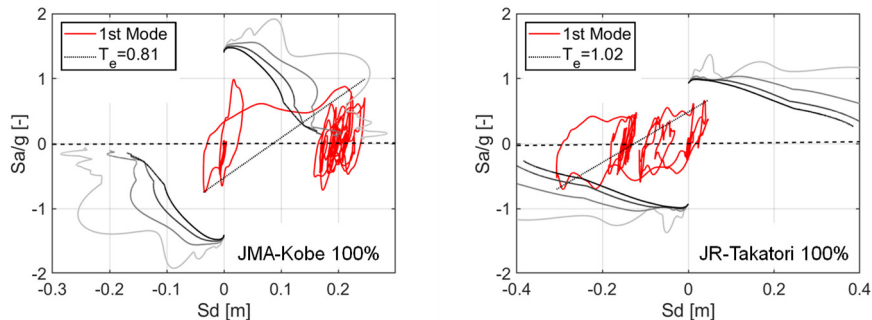
Fig. 18 Adopted mode vectors / JMA-Kobe 100% / X-direction



(1) A-building / Phase 1 (Base-isolation system) / X-direction



(2) A-building / Phase 2 (Fixed-foundation system) / X-direction



(3) B-building / Phase 1 (Soil-foundation system) / X-direction

Fig. 19 Comparison of test results and Acceleration Displacement Response Spectra

6. Conclusions

The 2019 full-scale shake table test was planned for current and future wood dwellings. The current Japanese seismic design guidelines were applied to three-story wood buildings. Two Grade-3 index buildings were prepared. One adopted the Post-and-Beam Structure (A-building), and the other the Shear-Wall structure (B-building). A-building with a fixed foundation had a maximum inter-story drift larger than 0.03 rad when subjected to JMA-Kobe 100%. On the other hand, B-building, which adopted the soil foundation, had an inter-story drift limited to less than 0.018 rad when subjected to the same JMA-Kobe 100%. The sliding displacement reached 250 mm at the foundation, while the upper structure showed input loss. These tests indicated that the upper structure possessing the Japanese Grade-3 capacity can induce sliding at the foundation, and result in the upper limit to seismic forces in the upper structure. Flexible pipelines should be installed in such buildings. The proposed base isolation system had successful results including the performance to keep



furniture and equipment safe in rooms. The seismic responses of the test buildings were reasonably assessed in the Acceleration Displacement Response Spectra format. This format can be a spine in future design practice. The resilience capacity enhancement of wood dwellings should be continuously discussed in terms of a holistic methodology containing all structural and nonstructural systems.

7. Acknowledgements

This work is supported by the Tokyo Metropolitan Resilience Project of the National Research Institute for Earth Science and Disaster Resilience (NIED). Collaboration on earthquake engineering research using E-Defense and NHERI facilities is proceeding continuously. Construction of the test buildings was managed by ICHIJO Co., Ltd. The relevant test affairs were administrated by the Graduate School of Environmental Studies, Nagoya University and E-Defense, NIED.

8. References

- [1] T. Nagae, S. Uwadan, K. Takaya, C. Yenidogan, S. Yamada, H. Kashiwa, K. Hayashi, T. Takahashi, T. Inoue (2020): Sliding-rocking combined actions at base foundation influencing global and local deformations of upper wood structure. *17th World Conference on Earthquake Engineering, 17WCEE*, Paper No. C002277
- [2] T. Takahashi, S. Uwadan, T. Nagae, C. Yenidogan, S. Yamada, H. Kashiwa, K. Hayashi, T. Inoue (2020): Stiffness, ultimate strength capacity and cyclic loading deterioration characteristics of two different wood-structure dwellings following the current Japanese practice. *17th World Conference on Earthquake Engineering, 17WCEE*, Paper No. C002285
- [3] C. Yenidogan, T. Takahashi, T. Nagae, T. Inoue (2020): Seismic performance evaluation of a base isolated P&B structure though full-scale shake table tests. *17th World Conference on Earthquake Engineering, 17WCEE*, Paper No. C004350
- [4] Y. Kawamata, T. Takahashi, T. Nagae (2020): Damage mechanism of PVC drainage pipe connected to house with high seismic performance. *17th World Conference on Earthquake Engineering, 17WCEE*, Paper No. C002097
- [5] C. Yenidogan, R. Nishi, S. Uwadan, T. Nagae, T. Takahashi, T. Inoue, K. Kajiwara (2020): Full-scale testing of a two-story P&B shearwall assembly under dynamic loading test protocol. *17th World Conference on Earthquake Engineering, 17WCEE*, Paper No. C003236
- [6] Y. L. Chung, C. Y. Ku, J. Chen, T. Nagae, K. Kajiwara (2020): Preliminary dynamic response characterization tests-III: South NCREE multi-directional shake table test for the seismic performance evaluation of the freestanding structures. *17th World Conference on Earthquake Engineering, 17WCEE*, Paper No. C002696
- [7] K. Hayashi, A. Yamada, Y. Komiya, T. Nagae (2020): Cost-effective smart sensing technologies to monitor the residential building systems. *17th World Conference on Earthquake Engineering, 17WCEE*, Paper No. C002857
- [8] M. Koliou, M. Aghababaei, T. Nagae, C. Pantelides, K. L. Ryan, A. Barbosa, S. Pei, J. W. van de Lindt, S. Dashti (2020): Rapid damage assessment procedure to collect, process and analyze data for monitoring of full-scale tests. *17th World Conference on Earthquake Engineering, 17WCEE*, Paper No. C002971